HEFAT2008
6th International Conference on Heat Transfer, Fluid Mechanics and Thermodynamics
30 June to 2 July 2008
Pretoria, South Africa
Paper number: CG2

NUMERICAL STUDIES OF COMBIED MULTIPLE SHELL-PASS SHELL-AND-TUBE HEAT EXCHANGERS WITH HELICAL BAFFLES

Guidong Chen, Min Zeng, Qiuwang Wang*

State Key Laboratory of Multiphase Flow in Power Engineering,
Xi'an Jiaotong University, Shaanxi, Xi'an 710049, China
*Corresponding author wangqw@mail.xjtu.edu.cn

ABSTRACT

In order to simplify the manufacture and improve the heat transfer performance, we have invented a combined multiple shell-pass shell-and-tube heat exchanger. The novel combined multiple shell-pass shell-and-tube heat exchanger (CM-STHXs) with continuous helical baffles in the outer shell-pass and other different baffles in the inner shell-pass was compared with conventional STHX with segmental baffles by Computational Fluid Dynamics method. The numerical results show that, under the same mass flow rate M and the same overall heat transfer rate Q_m in the shell side, the CM-STHX with discontinuous helical baffles in the inner shell-pass has the lowest overall pressure drop DP, which was 13% lower than that of the segmental baffled STHX; The heat transfer rate Q_m of the CM-STHX with discontinuous helical baffles in the inner shell-pass is about 2% and 12% higher than those of the CM-STHX with segmental baffles and disk-and-doughnut baffles in the inner shell-pass. The CM-STHX with discontinuous helical baffles in the inner shell-pass has a much better heat transfer performance and can be used to replace the conventional STHX with segmental baffles in industrial applications to save energy, reduce cost and prolong the service life.

Keywords: continuous helical baffle, disk-and-doughnut baffle, discontinuous helical baffle, combined multiple shell-pass heat exchanger

NOMENCLATURE

A	[m^2]	heat transfer area, $N_t \pi D_t L$
c_i	[-]	coefficients in the k-ε turbulence model
C_p	[J/kg K]	specific heat
D_e	[mm]	hydraulic diameter
D_{in}, D_{out}	[mm]	diameters of inlet tube and outlet tube
D_{is} ,D_{os}	[mm]	diameters of inner and outer shell
DP	[Pa]	overall pressure drop
D_t	[mm]	diameter of heat exchange tubes
DP_s,DP_h	[Pa]	overall pressure drop of the segmenatal baffled and the combined mutiple shell-pass SHTX
h	[W/m^2K]	average heat transfer coefficient, $q_m/\Delta T$
H_b	[mm]	pitch of baffles
k	[m^2/s^2]	turbulent fluctuation kinetic energy
L	[mm]	tube length
M	[kg/s]	mass flow rate
N_t	[-]	tube number
P_{out}	[Pa]	outlet pressure
Q_m	[W]	overall heat transfer rate, $C_p M (T_{out}-T_{in})$
x,y,z	[mm]	coordinates
Re	[-]	Reynolds number, $\rho u_m D_e /\mu$
ΔT	[℃]	log mean temperature difference, $\Delta T = (T_{out}-T_{in})/\ln[(T_w-T_{in})/(T_w-T_{out})]$
T_f	[K]	average temperature of fluid, $T_f=(T_{in}+T_{out})/2$
T_{in}	[K]	inlet temperature
T_{out}	[K]	outlet temperature
T_w	[K]	tube wall temperature
u, v, w	[m/s]	velocities in different directions
x^+ , y^+	[-]	non-dimensional distance from the wall

Greek symbols

β	[º]	helix angle, ,β=atan($2H_b/\pi D_{os}$)
ρ	[kg/m^3]	density of material
λ	[W/ m K]	thermal conductivity of material
Γ	[-]	generalized diffusion coefficient
ε	[m^2/s^3]	turbulent kinetic energy dissipation rate
μ	[kg/m s]	dynamic viscosity of fluid
ϕ	[-]	variables in generalized equations

INTRODUCTION

Heat exchangers play an important role in the fields of oil refining, chemical engineering, environmental protection, and electric power generation, et.al. Among different types of heat exchangers, shell-and-tube heat exchangers (STHXs) (as shown in Fig.1) have been commonly used in industries [1]. Master et

al. [2] indicated that more than 35–40% of heat exchangers are of the shell-and-tube type, and this is primarily due to the robust construction geometry as well as easy maintenance and possible upgrades. Plenty of studies pointed out that heat transfer effectiveness of STHXs can be improved by using baffles in the shell side.

For many years, various types of baffles have been designed, for example, the conventional segmental baffles with different arrangement , the deflecting baffles, the overlap helical baffles, the rod baffles and so on[3-5].They have been used to enhance the heat transfer performance and maintain a reasonable pressure drop for the heat exchangers. The most commonly used segmental baffles make the fluid flow in a tortuous, zigzag manner across the tube bundle in the shell side. It improves the heat transfer by enhancing turbulence and local mixing on the shell side of the heat exchanger. However, the traditional STHX with segmental baffles have many disadvantages, (1) high pressure drop on the shell side due to the sudden contraction and expansion of the flow in the shell side, and the fluid impinging on the shell walls caused by segmental baffles; (2) low heat transfer efficiency due to the flow stagnation in the so-called "stagnation regions," which are located at the corners between baffles and shell wall; (3) low shell side mass velocity across the tubes due to the leakage between baffles and shell wall caused by inaccuracy in manufacturing tolerance and installation; (4) short operation time due to the vibration caused by shell side flow normal to tube banks. When the traditional segmental baffles are used in STHXs, higher pumping power is often needed to offset the higher pressure drop under the same heat load. But segmental baffles are still widely used in industries, because they have a simply manufacture processing.

Helical baffles offer a possible alternative to segmental baffles by circumventing the aforementioned problems of conventional segmental baffles, they are accepted by their outstanding advantages including: (1) improving shell side heat transfer, (2) a lower pressure drop for a given mass flow rate, (3) reduced bypass effect, (4) reducing shell side fouling and preventing flow-induced vibration. Lutuha and Nemcansky [6] installed helical baffles in tubular heat exchangers and evaluated the improvement in the overall heat exchanger performance and found that heat transfer coefficient can be increased markedly by helical baffles. Stehlik et al. [7] carried out a study of correction factors for STHX with segmental baffles as compared to helical baffles. Kral et al. [8] discussed the performance of shell-and-tube heat exchangers with helical baffles using the results of tests conducted on units with various baffles geometries. The effectiveness of heat exchangers with helical baffles is proven on test units and in industry applications. Wang et al. [9, 10] have experimentally studied the influences of block plates and the helical angle on the performance of heat transfer and pressure drop in the SHTXs with overlap helical baffles. The results showed that under the same mass flow rate, the block plate increase the heat transfer coefficient by 15%. Under the same pressure drop, the heat transfer coefficient of heat exchanger without block plate is better than that with block plate. Zhang and Wang [11] have numerically studied the flow performance in shell side of STHX with discontinuous helical baffles.

Most of these helical baffles mentioned above are formed by lapped over fans or oval shaped plates, which are easy to be manufactured. These helical baffles are normally arranged by a central pole and the volume of the central pole is relatively small. However, serious leakage is induced by the triangle zones and it reduces the heat transfer coefficient of the STHX [12]. To overcome the above defects, Wang et al. [5, 13，17] have introduced a manufacture technique for continuous helical baffles and found that the heat exchangers with continuous helical baffles have a better performance than STHXs with segmental baffles and discontinuous helical baffles. Peng et al. [14] carried out an experimental investigation on heat exchanger with continuous helical baffles. The results indicated that heat transfer coefficient of the heat exchanger with continuous helical baffles was nearly 10% higher than that of the heat exchanger with segmental baffles under the same shell side flow rate. Xie et al. [15, 16] applied the genetic algorithm method to optimize STHX with helical baffles. But difficulties in manufacturing continuous helical baffles stop its popularization.

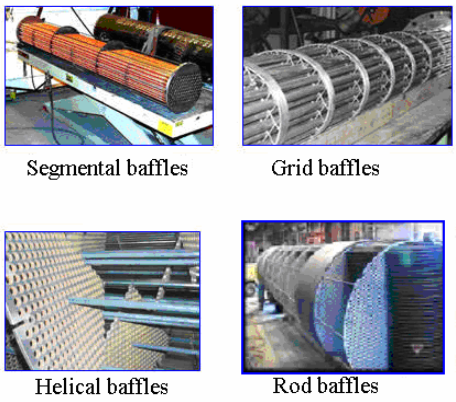

Fig.1 Various types of shell-and-tube heat exchanger

The above literature about STHX with discontinuous or continuous helical baffles is single shell-pass. To make full use of the advantages of continuous baffles, save more space, increase compactness of the heat exchangers and prolong the service time of STHX, Wang et al. [18-21] have invented a kind of combined multiple shell-pass heat exchanger with continuous helical baffles (CM-STHX) (as shown in Fig.2).This CM-STHX separates the shell side into several individual shell-pass. As to each individual shell-pass, the flow area is reduced, the velocity of the fluid is increased and the heat transfer performance can have a great improvement. In addition, the continuous helical baffles can reduce the pressure drop and mitigate fouling in the shell side. Moreover, the CM-STHXs can avoid the difficulties in manufacturing continuous helical baffles with a small scale inner helix.

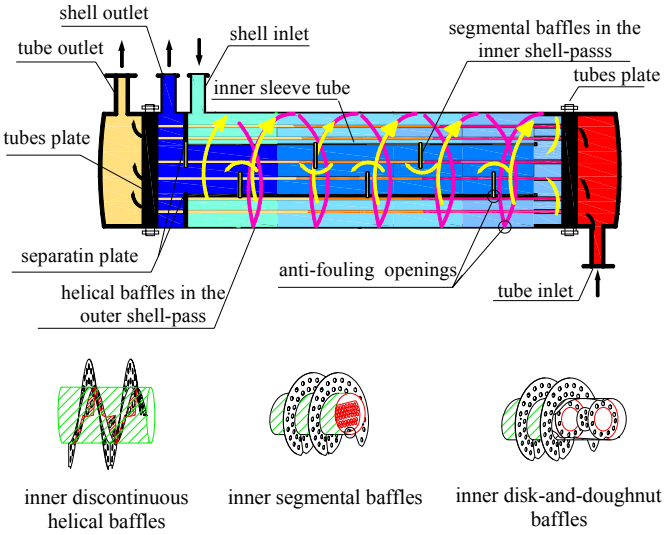

Fig.2 Schematic of the CM-STHX with continuous helical baffles [18,19,20]

In this study, the combined multiple shell-pass STHX with continuous helical baffles in the outer shell-pass, discontinuous helical baffles, segmental baffles and disk-and-doughnut baffles in the inner shell-pass were studied. At the same time a conventional STHX with segmental baffles was used for comparison. The Computational Fluid Dynamics (CFD) commercial software Fluent was used to study the flow and heat transfer characteristics in the shell side. All computations were performed on a personal computer with 8GB RAM and Intel® Core™ 2.40GHz CPU.

PHYSICAL MODEL

The physical model of the CM-STHX to be studied is presented in Fig.3. They have two shell passes in the shell side, the inner shell-pass and the outer shell-pass, which are separated by a sleeve tube. The inner shell-pass is set with segmental baffles, discontinuous helical baffles or disk-and-disk-and- doughnut baffles, the outer shell-pass is constructed by complete continuous helical baffles. The inner shell-pass and the outer shell-pass are joined together at one end of the shell side.

The material of the sleeve tube is steel with σ=2mm thickness, which has a density ρ=8030kg/m^3, thermal conductivity λ=16.27W/ (m K), specific heat C_p =502.48 J/ (kg K). The material of the heat exchange tubes and baffles is aluminum, which has a density ρ=2719kg/m^3, thermal conductivity λ= 202.4 W/ (m K), specific heat C_p =871J/ (kg K). The working fluid is water, whose thermal properties depend on the temperature. Detailed geometrical parameters of the computation models can be observed in Fig.3.

GOVERNING EQUATIONS

In order to simulate the flow and heat transfer in the shell side of STHXs, 3-dimensional Realizable k-ε turbulence model is applied. The generalized equation for different variables is as follows [22]:

$$div(\rho\vec{V}\phi) = div(\Gamma_\phi grad\phi) + S_\phi \qquad (1)$$

where ϕ stands for different variables, Γ stands for the corresponding generalized diffusion coefficient and S stands for the corresponding source term.Standard wall function is adopted near the wall and the range of the dimensionless length x^+ or y^+ is $10< x^+(y^+) <100$.

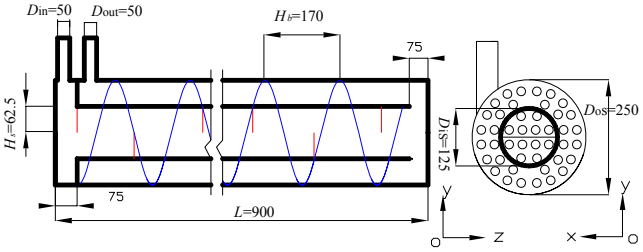

(a) CM-STHX with continuous helical baffles in outer shell pass

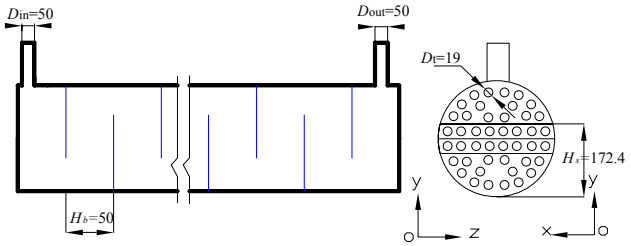

(b) Conventional STHX with segmental baffles

Fig. 3 Geometrical parameters of the STHX models (Unit: mm)

BOUNDARY CONDITIONS

The boundary conditions are described as follows:

(1) The shell inlet:

u=w=0, v=const (uniform inlet velocity),

T_{in}=298K (20 °C) (uniform inlet temperature)

The inlet turbulent kinetic energy k was calculated using:

$$k = \frac{3}{2} I^2 v^2$$

where I is the inlet turbulence intensity, I =10%.

The inlet dissipation ε was calculated using:

$$\varepsilon = \frac{c_\eta \rho k^2}{\mu_t}$$

where c_η is the turbulence coefficients, μ_t is the eddy viscosity.

(2) The shell outlet:

$$\frac{\partial u}{\partial n}=\frac{\partial v}{\partial n}=\frac{\partial w}{\partial n}=0$$

$$\frac{\partial T}{\partial n}=0$$

$$\frac{\partial k}{\partial n}=0,\frac{\partial \varepsilon}{\partial n}=0$$

where n is normal vector of outlet plane.

(3) The heat exchange tube wall surfaces:

$u=v=w=0$

T_w =373K (100 °C) (hot tube walls)

(4) The outer shell-pass walls

$u=v=w=0$

$\frac{\partial T}{\partial n}=0$ (thermal insulation walls)

(5) The sleeve tube surface:

$u=v=w=0$

(6) The baffle walls:

$u=v=w=0$

Due to the conjugated heat transfer characteristics between the baffle walls surface, sleeve tube wall surface, shell wall surface and the fluid, the boundary conditions for thermal fields do not need to be specified on the interior of baffle walls surface, the sleeve tube walls surface and the shell wall surface.

NUMERICAL METHODS

The SIMPLE algorithm and the second order upwind scheme are used for the numerical simulation. As the convergence criterion, the sum of the normalized absolute residuals in each control volume for the flow variables are controlled to be less than 10^{-5} and 10^{-7} for energy variables. The CUP time of a typical case is about 30 hours.

The Reynolds number is defined as

$$Re=\rho u_m D_e/\mu \quad (2)$$

where u_m, m/s, is the average velocity of fluid in shell side, which can be obtained from computation results. The hydraulic diameter $D_e=D_t$=19mm. ρ is the density of water, kg/m^3. μ is the dynamic viscosity of water, kg/(m s). ρ and μ are both determined by the average temperature of the working fluid $T_f=(T_{in}+T_{out})/2$.

The overall heat transfer rate Q_m can be calculated from:

$$Q_m=C_p M(T_{out}-T_{in}) \quad (3)$$

where T_{in} and T_{out} are the bulk inlet and outlet water temperatures, respectively. M is the mass flow rate of working fluid.

The average heat transfer coefficient h is defined as

$$h=Q_m/(\Delta T\ A) \quad (4)$$

where ΔT is log mean temperature difference and defined as ΔT= $(T_{out}-T_{in})/\ln[(T_w-T_{in})/(T_w-T_{out})]$. There are 44 heat exchange tubes arranged in shell side and the total heat transfer area A= $44\pi D_t L$.

GRID INDEPENDENCE

Due to the complex structure of the CM-STHXs, the computational domain is meshed with unstructured Tet/Hybrid grids (see Fig.4), which are generated by the commercial code GAMBIT. In order to ensure the accuracy of numerical results, a careful check for the grid independence of the numerical solutions was conducted. Four different grid systems are generated for the CM-STHX (Re=49129, M=10.92).

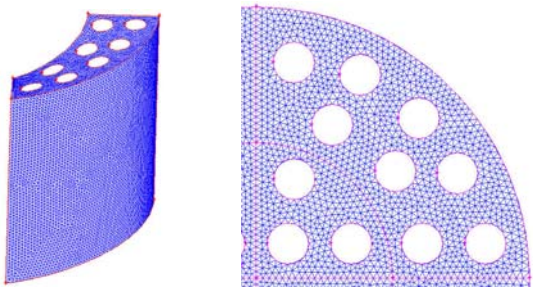

Fig. 4 Schematic diagrams of grid

The results are shown in Fig.5. It is found that the relative deviation of the average heat transfer coefficient under unit overall pressure drop h/DP between G3 and G4 is less than 2%. The relative deviation of the overall pressure drop DP between G3 and G4 is less than 3%. Therefore, the final grid system for the studied cases is G4.

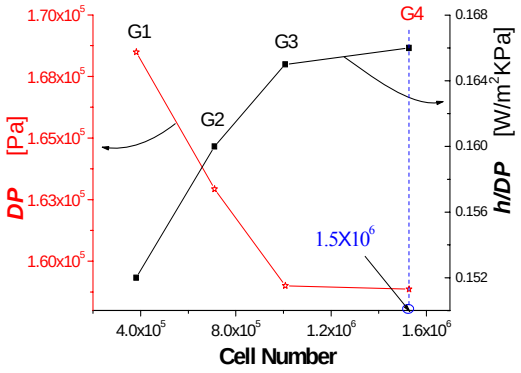

Fig.5 Results of different grid systems (Re=49129)

VALIDATION OF MODEL

The Kern method [22] is used to calculate the overall heat transfer rate Q_m in the shell side of the STHX with segmental baffles. The Esso method [22] is used to calculate the overall pressure drop DP in the shell side of the STHX with segmental baffles.

Comparisons of the present results with the prediction of correlations are shown in Fig.6. It is found that the average deviation of the overall heat transfer rate Q_m between present results and Kern design results is about 8.4%. It is acceptable in numerical simulation, so it can be concluded that the present model can give a close prediction in heat transfer performance. The average deviation and maximum deviation of the overall pressure drop DP between present results and Esso design results are 3.6% and 6.4%, respectively. The discrepancies between the simulation results and the experimental data can be explained as fellows. Kern and Esso methods are developed by certain experiments and they have taken account of the true situations of segmental baffled heat exchangers, but the simulation models neglect lots of factors such as bypass streams, leakage and the structure of the inlet and outlet. However, such an agreement should be regarded reasonable in engineering computation. The present models can give a close prediction in pressure drop characteristics.

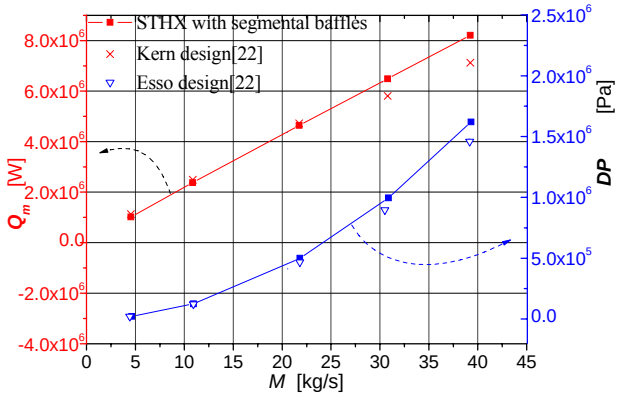

Fig.6 Comparisons of the present results with the prediction of correlations

RESULTS AND DISCUSSION

Temperature and velocity fields

The temperature and velocity distributions for the combined multiple shell-pass STHX with β=25° continuous helical baffles are shown in Figs.7-8, respectively. From Figs.7 (a, b, c, d), it can be observed that in the outer shell-pass of the CM-STHXs, temperatures increase evenly and smoothly. The difference of the temperature in each helix cycle is small. Because the continuous helical baffles and more heat exchange tubes located in the outer shell-pass, the working fluid has about 45℃ increase in the outer shell-pass and about 16℃increase in the inner shell-pass. From this point, the inner shell-pass has a relatively poor performance on heat transfer.

It can be seen from Figs.8 (a, b, c, d), as to the inner shell pass, disadvantages of segmental baffles, discontinuous helical baffles and disk-and-doughnut baffles can not be erased completely in these CM-STHXs. There are “stagnation regions” (marked by “S”) in the inner shell-pass of the CM-STHX with segmental baffles in the inner shell-pass. Stagnation regions have a low local heat transfer coefficient, because it can not exchange heat with the “main streams” (marked by “M”) freely. Due to the same reason mentioned above, temperatures of these stagnation regions are higher than those of the activity regions nearby; There are seriously leakage streams existed in the inner shell-pass of the CM-STHX with discontinuous helical baffles in the inner shell-pass, so that lots of working fluid flowing through the shell-pass without rush across the heat exchange tubes; “Stagnation zones” also effect heat transfer between heat exchange tubes and working fluid in the CM-STHX with disk-and-doughnut baffles in the inner shell pass.

Take the advantages of continuous helical baffles into consideration, it is valuable to separate the shell side into two different shell passes. The existence of inner shell-pass increases the scale of the inner helix and simplifies the manufacturing of continuous helical baffles. It also makes use of the space in the central pole, which is used to form the inner helix in the single shell pass STHX with continuous helical baffles. Segmental baffles, discontinuous helical baffles and disk-and-doughnut baffles are still better choice for the inner shell pass, because they can be manufactured and installed easily in a relatively small space. As can be seen from Fig.7 (d) and Fig.8 (d), in the STHX with segmental baffles, the fluid flows cross the heat exchange tubes and rushes toward the shell and baffles in a tortuous, zigzag manner. Back flow regions formed at the place where the baffles are attached to the shell wall.

Heat transfer and pressure drop characteristics

Variation of the overall heat transfer rate Q_m vs. mass flow rate M in the shell side is shown in Fig. 9. It can be found that the overall heat transfer rates Q_m of all STHXs are linear with the mass flow rate M. The maximum deviation of the overall heat transfer rate Q_m between these STHXs is less than 0.8%. From this point, it can be assumed that these SHTXs have the same overall heat transfer rate Q_m under the same mass flow rate M in the computations.

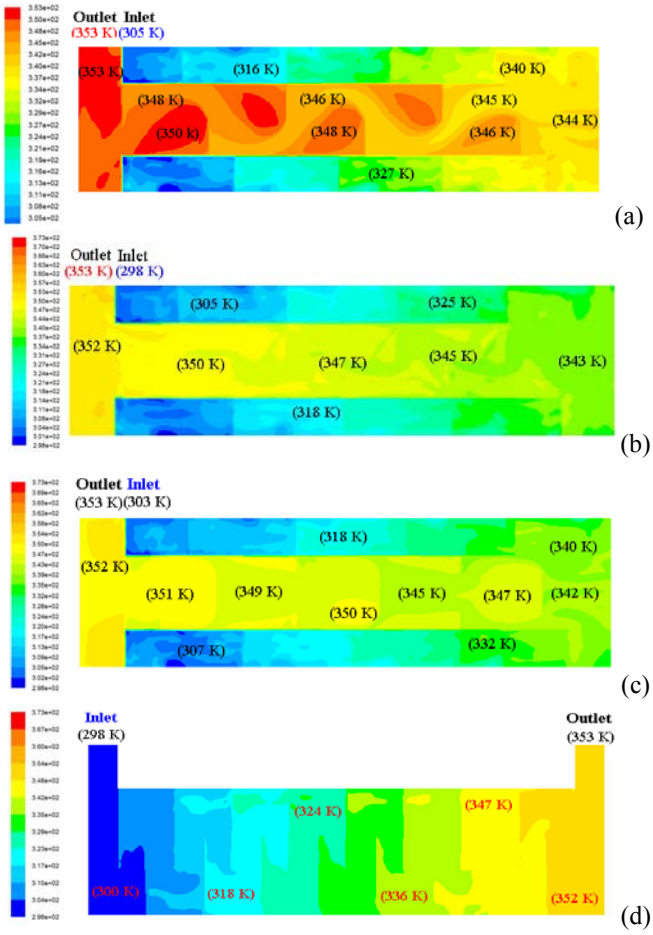

Fig. 7 Temperature distributions in the x-z sections (β=25°,M=4.3kg/s) (Unit: K)

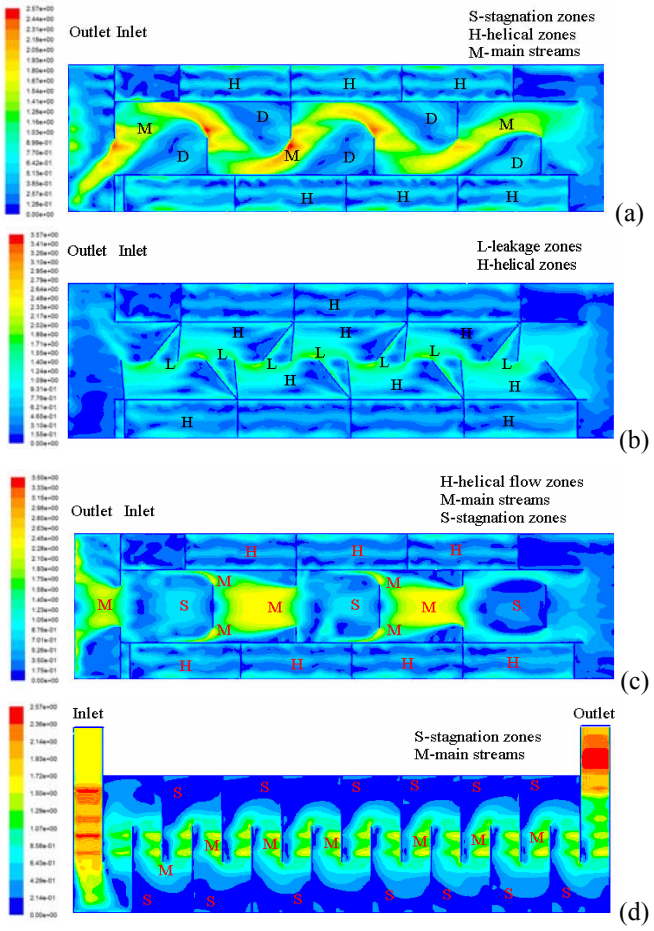

Fig.8 Velocity distributions in the x-z sections (β = 25°,M=4.3kg/s) (Unit: m/s)

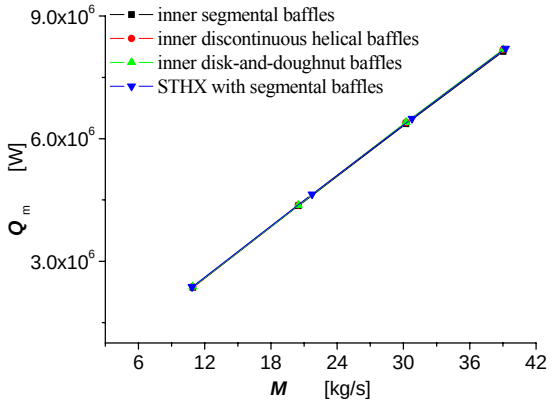

Fig. 9 Variation of Q_m vs. M (β = 25°)

Variation of the overall pressure drop DP vs. mass flow rate M in the shell side is shown in Fig. 10. It is found that the overall pressure drop DP has a great increase with the increase of the mass flow rate M in these STHXs. The overall pressure drop DP in the STHX with segmental baffles is 11.5% and 13.0% higher than those of the CM-STHXs with segmental and discontinuous helical baffles in the inner shell-pass under the same mass flow rate and the same overall heat transfer rate Q_m, respectively. However, the pressure drop of the CM-STHX with disk-and-doughnut baffles in the inner shell-pass is 6.0% higher than that of segmental baffled SHTX under the same mass flow rate and the same overall heat transfer rate Q_m. The same overall heat transfer rate Q_m is concluded from the analyses of Fig.9. From this point, it can be expected that the CM-STHX with segmental and discontinuous helical baffles in the inner shell-pass have a better heat transfer performance than that of the STHX with segmental baffles under the same mass flow rate M and the same overall pressure drop DP.

The variation of the overall heat transfer rate of the heat exchangers Q_m with the overall pressure drop DP is shown in Fig.11. The results indicate that in the lower overall pressure drop region, the heat transfer rate Q_m has a fast increasing with the increase of overall pressure drop, while in the high pressure drop region, this increase becomes smaller. For the same overall pressure drop, the difference of the overall heat transfer rate for

the STHXs is very small in the lower pressure drop region. However, in the higher pressure drop region, the overall heat transfer rate Q_m in the CM-STHXs with discontinuous helical baffles in the inner shell-pass is obviously higher than that in segmental baffled STHX at the same overall pressure drop DP. The heat transfer rate Q_m in it is about 8.0% higher than that in the STHX with segmental baffles.

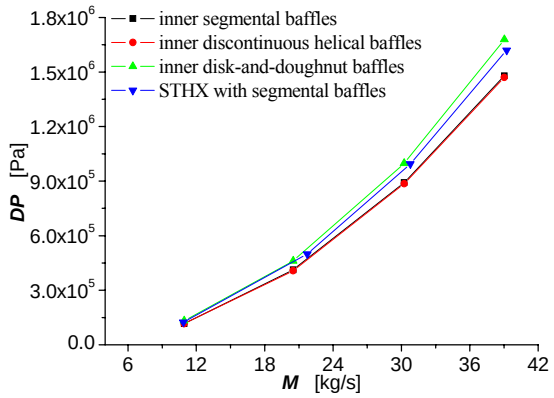

Fig. 10 Variation of DP vs. M (β = 25°)

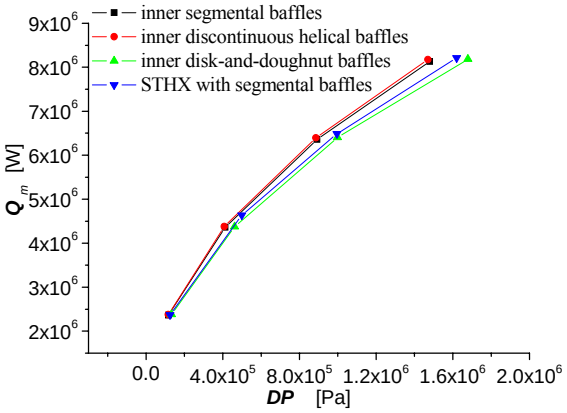

Fig. 11 Variation of Q_m vs. DP (β = 25°)

CONCLUSIONS

In the present paper, the combined multiple shell-pass STHXs with continuous helical baffles in the outer shell-pass and other kinds of baffles (segmental baffles, discontinuous baffles and disk-and-doughnut baffles) in the inner shell-pass (CM-STHXs) (helical angle β= 25°) were investigated by CFD method. The numerical simulation results are compared with the conventional STHX with segmental baffles. The conclusions are summarized as follows:

(1) In the CM-STHXs, the fluid temperature has a bigger increase in the outer shell-pass than that in the inner shell pass.

(2) The form of baffles in the inner shell pass has great influence on heat transfer. Under the same mass flow rate M and overall heat transfer rate Q_m, the overall pressure drop DP of the CM-STHX with discontinuous helical baffles or segmental baffles in the inner shell-pass is lower than that of segmental baffled STHX by 13% or 12% on average in the calculations.

(3) Under the same overall pressure drop DP in the shell side, the overall heat transfer rate Q_m of the CM-STHX with discontinuous helical baffles in the inner shell-pass is about 6% higher than that of conventional segmental baffled STHX.

ACKNOWLEDGMENTS

This work is supported by National Science and Foundation of China (Grant No. 50776068) and Program for New Century Excellent Talents in University of China (Grant No. NCET-04-0938).

REFERENCES

1. Gulyani B. B. Estimating number of shells in shell and tube heat exchangers: a new approach based on temperature cross, ASME J. Heat Transf, 122:566–571, 2000.
2. Master B.I., Chunangad K.S., Boxma A.J., Kral D., Stehlik P. Most frequently used heat exchangers from pioneering research to worldwide applications, Heat Transfer Engineering, 27(6):4-11, 2006.
3. Stehlik P. Wadekar V.V., Different strategies to improve industrial heat exchange, Heat Transfer Engineering, 23(6):36-48, 2002.
4. Wang L., Luo L.Q., Wang Q.W., Zeng M., Tao W.Q., Effect of inserting block planes on pressure drop and heat transfer in shell-and-tube heat exchangers with helical baffles, Journal of Engineering Thermophysics, 22(6):173-176, 2001. (In Chinese)
5. Wang Q.W.,Chen Q.Y., Peng B.T., Zeng M., Luo L.Q., Wu Y.N., Continuous helical baffled heat exchanger, China Patent, ZL 200510043033.5.
6. Lutuha J., Nemcansky J., Performance improvement of tubular heat exchangers by helical baffles, Trans. Inst. Chem.Eng. 68(A): 263–270, 1990.
7. Stehlik P., Nemcansky J., Kral D., Swanson L. W., Comparison of correction factors for shell-and-tube heat exchangers with segmental or helical baffles, Heat Transfer Eng., 15(1): 55–65, 1994.
8. Kral D., Stehlik, P., Van Der Ploeg H. J., and Master, B. I., Helical baffles shell-and-tube heat exchangers, Part 1: experimental verification, Heat Transfer Eng., 17(1): 93–101, 1996.
9. Butterworth D., Developments in shell-and-tube exchangers, Institution of Chemical Engineers Symposium Series, 1(129): 409-415, 1992.

10. Wang L., Luo L.Q., Wang Q.W., Zeng M., Tao W.Q., Effect of inserting block planes on pressure drop and heat transfer in shell-and-tube heat exchangers with helical baffles [J], Journal of Engineering Thermo physics, 22(6):173-176, 2001.(In Chinese)
11. Wang Q. W., Current status and development of shell side heat transfer enhancement of shell-and-tube heat exchangers with helical baffles [J], Journal of Xi'an Jiaotong University, 38(9):881-886, 2004. (In Chinese)
12. Zhang D.J., Wang Q.W., et al. Numerical simulation of flow performance in shell side of shell-and-tube heat exchanger with discontinuous helical baffles, Proceedings of the second international symposium on Thermal Science and Technology, Beijing, Oct. 23-25, 181-185,2005.
13. Zeng M., Peng B.T., Yu P.Q., Chen Q.Y., Wang Q.W., Huang Y.P., Xiao Z.J., Experimental study of heat transfer and flow resistance characteristics for shell-and-tube heat exchangers with continuous helical baffles, Nuclear Power Engineering, 27(S1) :102-106, 2006.(In Chinese)
14. Peng B., Wang Q.W, Zhang C., Xie G.N., Luo L.Q., Chen Q.Y., Zeng M., An experimental study of shell-and-tube heat exchangers with continuous helical baffles[J]; Journal of Heat Transfer-Transactions of the ASME,129(10): 1425-1431, 2007.
15. Xie G. N., Wang Q.W., Zeng M., Luo L.Q. Heat transfer analysis for shell-and-tube heat exchangers with experimental data by artificial neural networks approach, Applied Thermal Engineering, 27(5-6): 1096-1104, 2007.
16. Xie G.N, Bengt S.D., Wang Q.W. Optimization of compact heat exchangers by a genetic algorithm, Applied Thermal Engineering, 28: 895–906, 2008.
17. Wang Q.W., Zhang D.J., Zeng M., Wu Y.N., A combined shell-and-tube helical baffled heat exchanger, China Patent, CN101013009, 2007.
18. Wang Q.W., Chen Q.Y., Zeng M., Wu Y.N., Gao Q., A combined multiple shell-pass shell-and-tube helical baffled heat exchanger, China Patent, CN101021394, 2007.
19. Wang Q.W., Investigation on novel combined multi-shell-pass shell-and-tube heat exchangers with helical baffles[C], Workshop on advances in compact and micro heat exchangers for sustainable development, IIT Delhi, India, January 7-8, 2008 .(Keynote)
20. Wang Q. W., Chen Q.Y., Zhang D.J., Zeng M., Wu Y.N., Gao Q., A single shell side or multiple shell-pass shell-and-tube heat exchanger with helical baffles, US Patent, Application number: 11966256, 2007.
21. Wang Q.W., Chen Q.Y., Zeng M., Wu Y.N., Luo L.Q., A multiple shell-pass shell-and-tube helical baffled heat exchanger, China Patent, 200610041949.1.2006.
22. Tao W.Q., Numerical heat transfer, Xi'an Jiaotong University Press, 2002. (In Chinese)
23. Kuppan T., Heat exchangers design handbook. New York: Marcel Dekker, Inc., 2002.